Research article

# Ring-opening polymerization of lactides and ε-caprolactone catalyzed by Zn(II) aryl carboxylate complexes supported by 4-pyridinyl schiff base ligands

Damilola C. Akintayo [a], Wisdom A. Munzeiwa [a,b], Sreekantha B. Jonnalagadda [a], Bernard Omondi [a,*]

[a] School of Chemistry & Physics, University of KwaZulu-Natal, Westville Campus, Private Bag X54001, Durban, 4000, South Africa
[b] Chemistry Department, Bindura University of Science Education, Private Bag 1020, Bindura, Zimbabwe

ABSTRACT

Synthesis and catalytic studies of aryl carboxylate Zn (II) complexes is reported. Reaction of substituted (*E*)-*N*-phenyl-1-(pyridin-4-yl)methanimine with a methanolic solution of Zn $(CH_3COO)_2$ and substituted aryl carboxylate co-ligands gave heteroleptic Zn(II) complexes; [Zn $(C_6H_5COO)_2$(**L1**)]$_2$ (**1**), [Zn($C_7H_7COO)_2$(**L1**)]$_2$ (**2**), [Zn (4-F-$C_6H_4COO)_2$(**L1**)]$_2$ (**3**), [Zn $(C_6H_5COO)_2$(**L2**)]$_2$ (**4**), [Zn($C_7H_7COO)_2$(**L2**)]$_2$ (**5**), [Zn (4-F-$C_6H_4COO)_2$(**L2**)]$_2$ (**6**), [Zn $(C_6H_5COO)_2$(**L3**)]$_2$ (**7**), [Zn($C_7H_7COO)_2$(**L3**)]$_2$ (**8**), [Zn (4-F-$C_6H_4COO)_2$(**L3**)]$_2$ (**9**). The molecular structures of complexes **1** and **4** are dinuclear with the zinc atom in complex **1** adopting a distorted trigonal bipyramidal geometry in a bi-metallacycle while complex **4** is square pyramidal where all four benzoate ligands bridge the zinc metals in a paddle wheel arrangement. All complexes successfully initiated mass/bulk ring-opening polymerization (ROP) of ε-caprolactone (ε-CL) and lactides (LAs) monomers with or without alcohol co-initiators at elevated temperatures. Complexes **1**, **4** and **6** containing the unsubstituted benzoate co-ligands were the most active in their triad; with complex **4** being the most active ($k_{app}$) of 0.3450 h$^{-1}$. The physicochemical properties of the polymerization products of ʟ-lactide and *rac*-lactide in toluene revealed melting temperatures (T$_m$) between 116.58 °C and 188.03 °C, and decomposition temperatures between 278.78 °C and 331.32 °C suggestive of an isotactic PLA with a metal capped end.

## 1. Introduction

The depletion of petrochemical feedstock as well as the environmental threat posed by non-degradable polymers have led to the increased attention that polycaprolactone (PCL) and polylactides (PLA) have received [1, 2, 3, 4, 5]. Starting material used to produce PLA are acquired from biomass resources making them vital for a sustainable future [6]. The biodegradability of polyesters such as PCL and PLA is a major benefit for their use in agricultural [7, 8], pharmaceutical and biomedical field [9, 10]. These biodegradable aliphatic polyesters are largely obtained by ring opening polymerization (ROP) of respective monomers through a catalyzed route.

Metal complexes of main group elements such as calcium [11], lithium [12], magnesium [13] and aluminum [14] as well as other metals such as tin [15], zinc [16], copper [17], and cobalt [18], even lanthanides [19] have been investigated as catalyst in ROP of

---

cyclic esters monomers. Regardless of the toxicity posed by tin(II) octanoate [20], it has remained a standard catalyst used in industry in ROP studies. The development of new catalyst is hinged on the need to obtain biocompatible metal complexes that will combat the transesterification reactions faced by known catalysts to produce well-defined and neat polymers *via* different polymerization mechanisms.

Several types of ROP mechanisms have been put forward for different type of catalyst which can be nucleophilic or electrophilic. The most common ROP mechanisms for transition metal complexes are coordination insertion mechanism (CIM) and activated monomer mechanism (AMM). In CIM mechanism chain propagation proceeds *via* an intramolecular attack of a pre-coordinated lactone by the nucleophilic auxiliary ligand [21, 22]. In contrast, the AMM utilize a binary catalyst-co-initiator system, whereby the lactone is first coordinated to the metal center for activation and subsequently attacked by an external nucleophile which is the co-initiator. These two mechanisms have been complemented by experimental and computational data [23].

The increased attention received by zinc(II) and copper (II) complexes is hinged on their biocompatibility as well as their ease of synthesis. Carboxylate Zn(II) and Cu(II) complexes bearing *N*-donor ligands are characterized by their unique ability to coordinate in various modes depending on the electronic property of the ligands and the metal ionic character. Metal complexes bearing ancillary ligands such as (pyrazolylmethyl) pyridine [24, 25, 26], Bis(pyrazolylmethyl) pyridine [27, 28], Bis(3,5-dimethyl pyrazole) [29], (benzimidazolylmethyl) amine [30], formamidine [31, 32, 33, 34] have appeared in literature reports as catalyst/initiators for the ROP of ε-CL. Zeolitic imidazolate frameworks were also shown to catalyze the conversion of ε-caprolactone [35]. These organometallic complexes can be synthesized utilizing two approaches namely solution based and solid state, synthesis.

Solution based approaches utilizes organic solvents where the reactant components are dissolved to facilitate maximum interaction between the ions and the chelating ligands. The major glitch in such methods is long reaction time, high energy, and solvent consumption [36]. There are concerns over the toxicity of organic solvents used. Synthesis can be done at room or at elevated temperatures by heating using various methods which include conventional heating and microwave radiation [37]. Solid state approach involves mechanochemical activation of a physical mixture of the metal salts and the ligands. The merits of the method include fast reactions, simple, no solubility and solvent coordination issues and regarded as "greener" alternative [38].

This report covers comprehensive structural characterization of carboxylate complexes of *N*-(pyridin-4-yl) methanimine ligands and their catalytic potency in ROP of ε-CL, ʟ-LA and *rac*-LA. The reaction kinetics and polymer end group analysis catalytic influence of Schiff base ligands and bridging carboxylate co-ligands steric and electronic properties effects were also discussed.
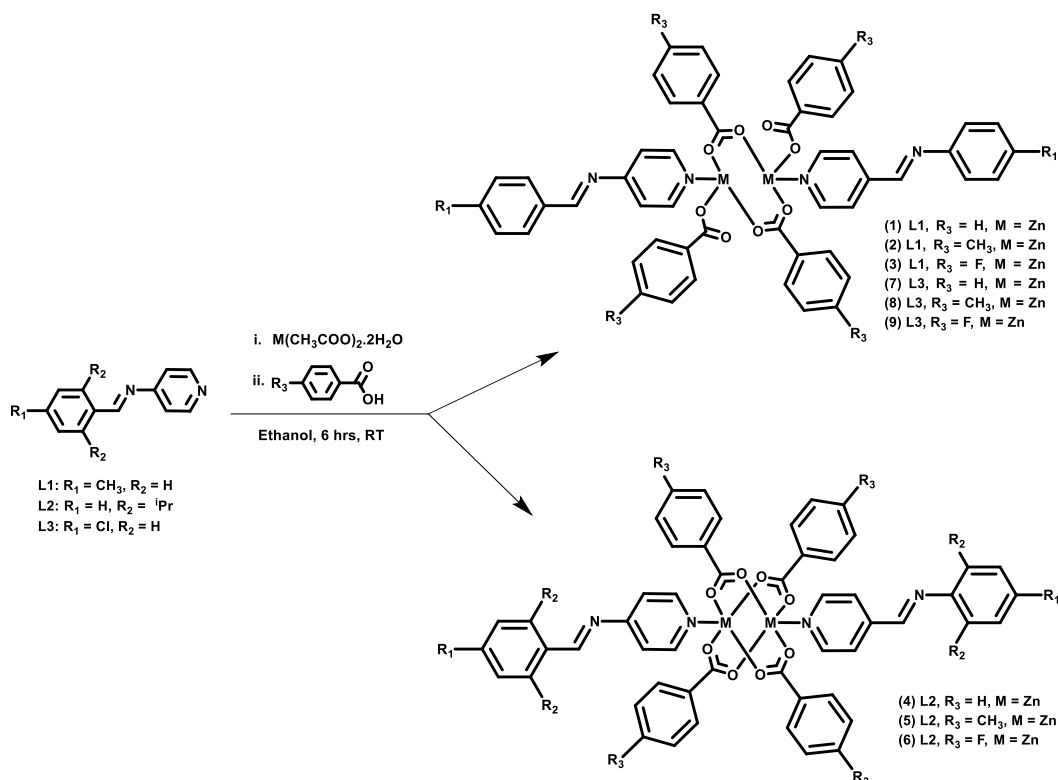


**Scheme 1.** Synthesis of zinc complexes.

## 2. Experimental

### 2.1. Materials

Aniline 99.5%, isonicotinaldehyde 99%, 4-chloroaniline 99%, 4-toluidine 99.6%, 2,6-diisopropylaniline 97%, ethanol 99.5%, $CDCl_3$ 99.8 atom % of D, diethyl ether 99.8% and dichloromethane 99% were obtained from Sigma Aldrich while argon and nitrogen gases, 5.0 technical grade were purchased from Airflex Industrial Gases, South Africa. All chemicals purchased were used without further purification, but the solvents were dried and distilled by conventional methods under inert atmospheric conditions before they were used.

### 2.2. Synthesis of Zn(II) aryl carboxylate complexes

The complexes were prepared in a one pot reaction between a metal (II) acetate, benzoic acid and the Schiff base ligand at room temperature (Scheme 1). In a typical reaction the metal (II) acetate (1 mmol) was stirred with the benzoic acid (2 mmol), in ethanol (15 mL) for 40 min at room temperature, after which a solution of the ligand was added as described for metal carboxylates [29, 39, 40].

#### 2.2.1. $[Zn(C_6H_5COO)_2(L1)]_2$ (1)

Complex **1** was synthesized using $[Zn(OAc)_2]$ (1.00 mmol), $C_6H_5COOH$ (2.00 mmol) and L1 (1.00 mmol) and isolated as a yellow solid. Yield = 80%, mp 223–224 °C. $^1$H NMR (400 MHz, $CDCl_3$): $\delta$ ppm 2.39 [s, 6H, $CH_3$], 7.22 [q, 8H, Ar], 7.32 [t, $J = 7.62$ Hz, 8H, Ar], 7.44 [t, 4H, Ar], 7.84 [d, $J = 5.92$ Hz, 4H, Ar], 8.10 [d, $J = 7.37$ Hz, 8H, Ar], 8.45 [s, 2H, HC═N], 8.89 [d, $J = 5.48$ Hz, 4H] $^{13}$C NMR (400 MHz, $CDCl_3$): $\delta$ ppm 174.28, 155.48, 150.09, 147.82, 144.88, 137.77, 132.99, 132.07, 130.54, 129.99, 127.88, 123.09, 121.11, 21.13. . IR: $\upsilon$ (cm$^{-1}$) 3059 $\upsilon$(C–H) str., 1636 $\upsilon$(C═O) *asym.* str., 1420 $\upsilon$(C═O) *sym.* str., 720 $\upsilon$ (M − O) str., 461 $\upsilon$ (M − N) str. ESI-TOF MS: *m/z* (%); [M + Na]$^+$ = 1029.8429. Anal. calcd for $C_{54}H_{44}N_4O_8Zn_2$: C, 64.36; H, 4.40; N, 5.56%. Found: C, 64.22, H, 4.43, N, 5.62%.

#### 2.2.2. $[Zn(C_7H_7COO)_2(L1)]_2$ (2)

Complex **2** was synthesized using $[Zn(OAc)_2]$ (1.00 mmol), $C_7H_7COOH$ (2.00 mmol) and L1 (1.00 mmol) and isolated as a yellow solid. Yield = 82%, mp 252–253 °C. $^1$H NMR (400 MHz, $CDCl_3$): $\delta$ ppm 2.36–2.39 [s, 18H, $CH_3$], 7.15 [d, $J = 8.00$ Hz, 8H, Ar], 7.22 [q, $J = 8.37$ Hz, 4H, Ar], 7.85 [d, $J = 5.54$ Hz, 4H, Ar], 8.01 (d, $J = 8.06$ Hz, 8H, Ar], 8.47 [s, 2H, HC═N], 8.87 [d, $J = 4.07$ Hz, 4H, Ar] $^{13}$C NMR (400 MHz, $CDCl_3$): $\delta$ ppm 174.43, 155.65, 151.20, 150.15, 147.87, 144.68, 142.59, 137.71, 130.64, 130.15, 129.99, 128.63, 123.01, 121.10, 21.60, 21.12. . IR: $\upsilon$ (cm$^{-1}$) 2924 $\upsilon$(C–H) str., 1602 $\upsilon$(CO) *asym.* str., 1400 $\upsilon$(C═O) *sym.* str., 778 $\upsilon$ (M − O) str., 439 $\upsilon$ (M − N) str. ESI-TOF MS: *m/z* (%); [M+Na]$^+$ = 1081.4037. Anal. calcd for $C_{58}H_{52}N_4O_8Zn_2$: C, 65.48; H, 4.93; N, 5.27%. Found: C, 65.52, H, 4.945, N, 5.43%.

#### 2.2.3. $[Zn(4-F-C_6H_4COO)_2(L1)]_2$ (3)

Complex **3** was synthesized using $[Zn(OAc)_2]$ (1.00 mmol), 4-F-$C_6H_4COOH$ (2.00 mmol) and L1 (1.00 mmol) and isolated as a yellow solid. Yield = 78%, mp 225–226 °C. $^1$H NMR (400 MHz, $CDCl_3$): $\delta$ ppm 8.88 [d, $J = 5.52$ Hz, 4H, Ar], 8.47 [s, 2H, HC═N], 8.08 [q, 8H, Ar], 7.86 [d, $J = 5.88$ Hz, 4H, Ar], 7.22 [t, 8H, Ar], 6.97 [t, $J = 8.59$ Hz, 8H, Ar], 2.39 [s, 6H, $CH_3$] $^{13}$C NMR (400 MHz, $CDCl_3$): $\delta$ ppm 173.24, 166.65, 164.15, 155.18, 150.00, 147,71, 145.14, 137.93, 132.99, 132.89, 130.03, 129.18, 123.18, 121.13, 114.97, 114.76, 21.12. IR: $\upsilon$ (cm$^{-1}$) 2936 $\upsilon$(C–H) str., 1636 $\upsilon$(C═O) *asym.* str., 1410 $\upsilon$(C═O) *sym.* str., 778 $\upsilon$ (M − O) str., 439 $\upsilon$ (M − N) str. ESI-TOF MS: *m/z* (%); [M+2Na]$^{2+}$ = 1125.3625. Anal. calcd for $C_{54}H_{40}F_4N_4O_8Zn_2$: C, 60.07; H, 3.73; N, 7.04%. Found: C, 60.17, H, 3.69, N, 6.95%.

#### 2.2.4. $[Zn(C_6H_5COO)_2(L2)]_2$ (4)

Complex **4** was synthesized using $[Zn(OAc)_2]$ (1.00 mmol), $C_6H_5COOH$ (2.00 mmol) and L2 (1.00 mmol) and isolated as a yellow solid. Yield = 82%, mp 170–171 °C. $^1$H NMR (400 MHz, $CDCl_3$): $\delta$ ppm 1.16–1.18 [s, 24H, $CH_3$], 2.83–2.90 [m, 4H, CH], 7.17 [q, 6H, Ar], 7.33 [d, $J = 7.58$ Hz, 4H, Ar], 7.45 [t, 2H, Ar], 7.87 [d, $J = 5.09$ Hz, 4H, Ar], 8.11 [d, $J = 7.30$ Hz, 4H, Ar] 8.21 [s, 2H, HC═N], 8.96 [s, 4H, Ar]. ]. $^{13}$C NMR (400 MHz, $CDCl_3$): $\delta$ ppm 174.04, 159.58, 159.55, 150.43, 148.20, 144.02, 143.96, 137.06, 131.89, 131.86, 130.45, 127.86, 124.99, 123.21, 122.93, 122.78, 118.60, 28.05, 23.40, 22.46. IR: $\upsilon$ (cm$^{-1}$) 2959 $\upsilon$(C–H) str., 1602 $\upsilon$(C═O) *asym.* str., 1399 $\upsilon$(CO) *sym.* str., 720 $\upsilon$ (M − O) str., 461 $\upsilon$ (M − N) str. ESI-TOF MS: *m/z* (%); [M+H]$^+$ = 1145.4896. Anal. calcd for $C_{64}H_{64}N_4O_8Zn_2$: C, 66.96; H, 5.62; N, 4.88%. Found: C, 66.85, H, 5.624, N, 4.97%.

#### 2.2.5. $[Zn(C_7H_7COO)_2(L2)]_2$ (5)

Complex **5** was synthesized using $[Zn(OAc)_2]$ (1.00 mmol), $C_7H_7COOH$ (2.00 mmol) and L2 (1.00 mmol) and isolated as a yellow solid. Yield = 82%, mp 176–178 °C. $^1$H NMR (400 MHz, $CDCl_3$): $\delta$ ppm 1.17–1.18 [s, 24H, $CH_3$], 2.38 [s, 12H, $CH_3$], 2.88 [m, 4H, CH], 7.16–7.18 [q, $J = 4.83$ Hz, 6H, Ar], 7.93 [d, $J = 5.27$ Hz, 4H, Ar], 8.06 [d, $J = 7.87$ Hz, 8H, Ar], 8.24 [s, 2H, HC═N], 8.97 [d, 8H, Ar]. ]. $^{13}$C NMR (400 MHz, $CDCl_3$): $\delta$ ppm 174.57, 159.57, 150.41, 148.21, 144.03, 142.75, 137.07, 130.69, 130.06, 128.68, 125.00, 123.22, 122.96, 28.07, 23.41, 21.62. IR: $\upsilon$ (cm$^{-1}$) 2959 $\upsilon$(C–H) str., 1602 $\upsilon$(CO) *asym.* Str., 1410 $\upsilon$(C═O) *sym.* Str., 778 $\upsilon$ (M − O) str., 439 $\upsilon$ (M − N) str. ESI-TOF MS: *m/z* (%); [M]$^+$ = 1203.5505. Anal. calcd for $C_{68}H_{72}N_4O_4Zn_2$: C, 67.83; H, 6.03; N, 4.65%. Found: C, 67.68, H, 6.00, N, 4.75%.

### 2.2.6. *[Zn(4-F-C₆H₄COO)₂(L2)]₂ (6)*

Complex **6** was synthesized using [Zn(OAc)₂] (1.00 mmol), 4-F-C₆H₄COOH (2.00 mmol) and L2 (1.00 mmol) and isolated as a yellow solid. Yield = 78%. Mp 184 °C. ¹H NMR (400 MHz, DMSO): $\delta$ ppm 1.16 [s, 24H, CH₃], 2.86 [m, 4H, CH], 6.94 [t, *J* = 8.46 Hz, 4H, Ar], 7.16 [m, 6H, Ar], 7.88 (d, *J* = 5.55 Hz, 4H, Ar], 8.05 [t, 4H, Ar], 8.20 [s, 2H, HC═N], 8.95 (d, *J* = 5.14 Hz, 4H, Ar]. ¹³C NMR (400 MHz, CDCl₃): $\delta$ ppm 159.29, 150.27, 148.09, 137.03, 132.03, 131.20, 127.26, 125.09, 123.24, 123.07, 28.08, 23.41, 22.46. IR: $\upsilon$ (cm⁻¹) 2969 $\upsilon$(C–H) str., 1636 $\upsilon$(CO) *asym.* Str., 1400 $\upsilon$(C═O) *sym.* Str., 778 $\upsilon$ (M − O) str., 427 $\upsilon$ (M − N) str. ESI-TOF MS: *m/z* (%); [M]⁺ = 1219.5040. Anal. calcd for C₆₄H₆₀F₄N₄O₈Zn₂: C, 63.01; H, 4.96; N, 4.59%. Found: C, 62.92, H, 5.04, N, 4.62%.

### 2.2.7. *[Zn(C₆H₅COO)₂(L3)]₂ (7)*

Complex **7** was synthesized using [Zn(OAc)₂] (1.00 mmol), C₆H₅COOH (2.00 mmol) and L3 (1.00 mmol) and isolated as a yellow solid. Yield = 82%, mp 222–223 °C. ¹H NMR (400 MHz, CDCl₃): $\delta$ ppm7.21 (4H, d, *J* = 8.52 Hz), 7.32 (8H, t, *J* = 7.60 Hz), 7.40 (4H, d, *J* = 8.52 Hz), 7.44 (4H, t, *J* = 7.34 Hz), 7.84 (4H, d, *J* = 5.72 Hz), 8.10 (8H, d, *J* = 7.60 Hz), 8.42 (2H, s), 8.92 (4H, d, *J* = 5.48 Hz). ¹¹³C NMR (400 MHz, CDCl₃): $\delta$ ppm116.43, 122.42, 123.17, 127.88, 129.12, 129.53, 130.53, 132.08, 133.01, 133.24, 144.37, 148.83, 150.22, 151.18, 156.93, 174.34. IR: $\upsilon$ (cm⁻¹) 3049 $\upsilon$(C–H) str., 1614 $\upsilon$(C═O) *asym.* Str., 1379 $\upsilon$(CO) *sym.* Str., 710 $\upsilon$ (M − O) str., 416 $\upsilon$ (M − N) str. ESI-TOF MS: *m/z* (%); [M+2Na]²⁺ = 1095.2750. Anal. calcd for C₅₂H₃₈Cl₂N₄O₈Zn₂: C, 59.56; H, 3.65; N, 5.34%. Found: C, 59.47, H, 3.73, N, 5.34%.

### 2.2.8. *[Zn(C₇H₇COO)₂(L3)]₂ (8)*

Complex **8** was synthesized using [Zn(OAc)₂] (1.00 mmol), C₇H₇COOH (2.00 mmol) and L3 (1.00 mmol) and isolated as a yellow solid. Yield = 82%, mp 248–249 °C. ¹H NMR (400 MHz, CDCl₃): $\delta$ ppm 2.35 (12H, s), 7.13 (8H, d, *J* = 7.96 Hz), 7.21 (4H, d, *J* = 8.60 Hz), 7.39 (4H, d, *J* = 8.60 Hz), 7.86 (4H, d, *J* = 5.72 Hz), 8.00 (8H, d, *J* = 8.00 Hz), 8.44 (2H, s), 8.93 (4H, d, *J* = 5.48 Hz). ¹³C NMR (400 MHz, CDCl₃): $\delta$ ppm 21.61, 122.46, 123.30, 128.65, 129.53, 130.02, 130.60, 133.28, 142.63, 144.58, 148.78, 156.86, 174.27. IR: $\upsilon$ (cm⁻¹) 3026 $\upsilon$(C–H) str., 1602 $\upsilon$(C═O) *asym.* Str., 1400 $\upsilon$(CO) *sym.* Str., 766 $\upsilon$ (M − O) str., 416 $\upsilon$ (M − N) str. ESI-TOF MS: *m/z* (%); [M+Na]⁺ = 1123.2943. Anal. calcd for C₅₆H₄₆Cl₂N₄O₈Zn₂: C, 60.89; H, 4.20; N, 5.07%. Found: C, 60.89, H, 4.301, N, 4.98%.

### 2.2.9. *[Zn (4-F-C₆H₄COO)₂(L3)]₂ (9)*

Complex **9** was synthesized using [Zn(OAc)₂] (1.00 mmol), 4-F-C₆H₄COOH (2.00 mmol) and L3 (1.00 mmol) and isolated as a yellow solid. Yield = 78%. Mp 229–230 °C. ¹H NMR (400 MHz, DMSO): $\delta$ ppm 7.21 (8H, t, *J* = 8.82 Hz), 7.37 (4H, d, *J* = 8.59 Hz), 7.50 (4H, d, *J* = 8.58 Hz), 7.93 (4H, d, *J* = 5.86 Hz), 8.02 (8H, q, *J* = 4.81 Hz), 8.72 (2H, s), 8.81 (4H, d, *J* = 5.81 Hz). ¹³C NMR (400 MHz, DMSO): $\delta$ ppm 115.08, 115.29, 123.13, 123.59, 129.73, 131.78, 132.54, 143.53, 149.62, 150.79, 151.50, 160.24, 163.20, 165.66, 171.20. IR: $\upsilon$ (cm⁻¹) 3083 $\upsilon$(C–H) str., 1636 $\upsilon$(CO) *asym.* Str., 1400 $\upsilon$(CO) *sym.* Str., 766 $\upsilon$ (M − O) str., 428 $\upsilon$ (M − N) str. ESI-TOF MS: *m/z* (%); [M+2Na]²⁺ = 1161.2722. Anal. calcd for C₅₂H₃₄Cl₂F₄N₄O₈Zn₂: C, 55.74; H, 3.06; N, 5.00%. Found: C, 55.68, H, 3.17, N, 5.10%.

## 3. General procedure for ROP of cyclic esters

The polymerization reactions were performed in a carousel reaction station, fitted with 12 tubes, a gas distribution system and a reflux unit. ε-CL (1.14 g, 0.01 mol) and the required amount of initiator, depending on the [M]: [I] ratio used, were weighed in a reactor tube and stirred at 110 °C. After the required reaction time, the reaction mixture was quenched by rapid cooling to room temperature and the crude product was analyzed by ¹H NMR spectroscopy in CDCl₃. The polymers were cleaned by first dissolving the crude product in CH₂Cl₂, followed by the addition of cold methanol. The white precipitate formed was altered and dried in vacuo. Polymer conversions were analyzed from the peak areas obtained from ¹H NMR spectroscopy and calculated using equation (1) for ε-CL monomer and equation (2) for LAs [41,42].

$$\frac{[Polymer]_t}{[Monomer]_o} \ x \ 100 = \frac{I_{4.0}}{(I_{4.0} + I_{4.2})} \ x \ 100 \tag{1}$$

$$\frac{[Polymer]_t}{[Monomer]_o} \ x \ 100 = \frac{I_{CH \ polymer}}{(I_{CH \ monomer} + I_{CH \ polymer})} \ x \ 100 \tag{2}$$

The catalytic activities of **4** towards ε-caprolactone (ε-CL) and ᴅ,ʟ-lactide polymerizations have been evaluated under different conditions. Polymerization of ε-caprolactone was carried out in bulk using a [monomer]: [initiator] ([M]: [I]) ratio of 100–400. For the polymerization of ᴅ,ʟ-lactide, the reaction was performed in toluene using a [M]: [I] ratio of 200.

### 3.1. *Molecular structure of complexes*

Single-crystals of complexes **1** and **4** were analyzed on a 'Bruker APEX-II CCD' diffractometer comprising of a low temperature Oxford Cryostream system. The selected crystals were retained at 100.0 K throughout the data collection exercise. Data reduction was performed using the *SAINT* [43] software and the scaling and absorption corrections were applied using the *SADABS* [44] multi-scan technique. Using Olex2 [45], the structure was solved with the ShelXT [46] structure solution program using Intrinsic Phasing and refined with the ShelXL [46] refinement package using Least Squares minimization. Non-hydrogen atoms were first refined

isotropically and then by anisotropic refinement with the full-matrix least squares method based on $F_2$ using *SHELXL* [23]. Crystallographic data and structure refinement parameters are given in Table 1.

## 4. Results and discussion

### 4.1. Synthesis and characterization

The Schiff base ligands were obtained by mechanochemically grinding isonicotinaldehyde with substituted anilines in a mortar and pestle. Mechanochemical offers a robust synthetic route where products are obtained in high yields, rapidly and much pure. This solvent free approach *via* grinding can result in generation of excessive heat which can lead to product isomerization and/or decomposition [36, 47]. Although sometimes this method is referred to as greener approach, in some cases solvents may be used for purification and isolation of the products. Purity of ligands was ascertained by $^1$H and $^{13}$C NMR and the spectra appear in Fig. S1, S2, S3, S4, S5 and S6.

One pot reaction of the pyridinyl Schiff base ligands, substituted and unsubstituted benzoic acids with zinc(II) acetates in methanol produced zinc carboxylates complexes in good yield (78–82%) as depicted in Scheme 1. All complexes were characterized by IR, NMR, mass spectrometry, UV–vis and elemental analysis. Mass spectroscopy and elemental analysis of all the complexes conforms to dinuclear carboxylate systems [Zn**Ln** (RCOO)$_2$]$_2$.

Distinctive ligand peaks after complexation to the zinc metal were observed with IR and NMR spectroscopies. The Schiff base ligands experienced a shift in the proton peaks of the pyridinyl moiety in the $^1$H NMR spectra (Fig. S7, S8, S9, S10, S11, S12, S13, S14 and-S15). IR and $^{13}$C NMR spectroscopies are known to provide valid evidence about the coordination modes of carboxylate complexes [48]. In the $^{13}$C NMR spectra (Fig. S16, S17, S18, S19, S20, S21, S22, S23 and S24), a peak around 173–174 ppm corresponds to the carboxylate carbonyl carbon coordinated in a bidentate fashion to the zinc metal. Bands corresponding to Zn—N$_{py}$ were observed between 416 and 461 cm$^{-1}$ and Zn–O at 710 - 778 cm$^{-1}$ in the IR spectra (Fig. S25, S26, S27, S28, S29, S30, S31, S32 and S33). The IR spectra of complexes **1**–**9** revealed intense bands between 1379 and 1420 cm$^{-1}$ for $\upsilon_{sym}$ (COO$^-$) and 1602–1636 cm$^{-1}$ for $\upsilon_{asym}$ (COO$^-$) (Fig. S25, S26, S27, S28, S29, S30, S31, S32 and S33) [32,49–51]. The $\Delta\upsilon$ ($\upsilon_{asym}$ − $\upsilon_{sym}$) values for all complexes are in the range 192–236 cm$^{-1}$ which is in consonance with asymmetrical bidentate bridging mode [52].

The substituents of the aryl carboxylate co-ligands had a bearing on the magnitude of $\Delta\upsilon$ obtained in all the complexes. Complexes **3**, **6** and **9** with an electron withdrawing fluoro on the carboxylate phenyl ring in their triad have the highest $\Delta\upsilon$ while **2**, **5** and **8** with an electron donating methyl were smaller than **1**, **4** and **7** having the unsubstituted benzoate ligands. Absorption electronic spectra of complexes **1**–**9** in chloroform analyzed between 220 and 440 nm afforded electronic absorption bands between 231 – 266 nm and

**Table 1**
Crystal data and structure refinement parameters for complexes **1** and **4**.

| Complex | 1 | 4 |
|---|---|---|
| Empirical formula | C$_{54}$H$_{44}$N$_4$O$_8$Zn$_2$ | C$_{64}$H$_{64}$N$_4$O$_8$Zn$_2$ |
| Formula weight | 1007.76 | 1147.92 |
| $T$/K | 150.01 | 100.01 |
| $\lambda$/Å | 0.71073 | 0.71073 |
| Crystal system | Monoclinic | Monoclinic |
| Space group | $C2/c$ | $P2_1/c$ |
| $a$/Å | 29.5190 (6) | 16.116 (3) |
| $b$/Å | 11.0215 (2) | 7.5994 (14) |
| /Å | 16.0324 (3) | 24.185 (4) |
| $\alpha$/° | 90 | 90 |
| $\beta$/° | 116.4460 (10) | 97.820 (9) |
| $\gamma$/° | 90 | 90 |
| $V$/Å$^3$ | 4670.20 (16) | 2934 (9) |
| Z | 4 | 4 |
| $\rho_{(calc)}$/g cm$^{-3}$ | 1.4332 | 1.299 |
| $\mu$/mm$^{-1}$ | 1.089 | 0.875 |
| F (000) | 2083.4 | 1200 |
| Size/mm$^3$ | 0.34 × 0.21 × 0.14 | 0.36 × 0.17 × 0.12 |
| θ range/° | 4 to 52.74 | 1.982 to 28.831 |
| Index ranges | −36 ≤ h ≤ 36 | −20 ≤ h ≤ 21 |
| | −13 ≤ k ≤ 13 | −10 ≤ k ≤ 10 |
| | −19 ≤ l ≤ 19 | −31 ≤ l ≤ 31 |
| Reflections collected | 22 453 | 33 458 |
| Independent reflections | 4720 [R (int) = 0.0242] | 7289 [R (int) = 0.0215] |
| Data/restraints/parameters | 4720/0/308 | 7289/0/370 |
| GooF | 0.833 | 1.028 |
| R indices [I > 2sigma(I)] $R_1$ w$R_2$ | 0.0268 | 0.0322 |
| | 0.0901 | 0.0696 |
| R indices (all data) $R_1$ w$R_2$ | 0.0334 | 0.0475 |
| | 0.0996 | 0.0748 |
| Largest diff. peak/hole/e Å$^{-3}$ | 0.34/−0.36 | 0.359/−0.448 |

322–340 nm allocated to π-π* and n-π* transition, respectively (Fig. 1).

### 4.1.1. Molecular structures of complexes 1 and 4

Complex **1** was formed by slow evaporation of a dcm/hex mixture (1:1) solution and **4** was gotten from recrystallization in methanol at room temperature. The molecular structures of complexes **1** and **4** are shown in Fig. 2a and b, while the selected crystallographic data is given in Table 2. Complexes **1** and **4** are di-nuclear species and the asymmetric unit is occupied by half a molecule with the other half generated by symmetry operation at the center of inversion between the zinc centers.

The zinc atoms in complex **1** adopts a distorted trigonal bipyramidal geometry (Fig. 2a) in a bi-metallacycle with the O–C–O of the two carboxylate ligands bridging the zinc metals with bond angles of 108.59 (5)° and 125.02 (14)° for O–Zn–O and O–C–O, respectively [31]. The two bridging carboxylate ligands have a Zn–O bond length of 1.9413 (11) Å and 1.9899 (12) Å [53,54]. The other two carboxylates form a *syn*-syn asymmetric chelate [30,55] with each zinc metal resulting in a Zn–O bond length of 1.9547 (12) Å and 2.5542 (13) Å. The Zn—$N_{py}$ bond length and N–Zn–O bond angles in this geometry ranges between 2.029(2) – 2.046(2) Å and 98.59(7) – 112.55(7)°, respectively (Table 1). Complex **4** adopts a square pyramidal geometry where all four benzoate ligands bridged the zinc metals in a paddle wheel arrangement (Fig. 2b). The four O atoms of the carboxylate occupy the base with a Zn–O bond length of 2.0624(12) – 2.0813(12) Å and the ligand pyridinyl N stands at the apex of the pyramid with a Zn—$N_{py}$ length of 2.0375 (14) Å and 2.0565 (13) Å.

## 5. Ring opening polymerization of cyclic esters

The initiation efficiency of the zinc complexes was examined for the polymerization of ε-CL, $_L$-LA and *rac*-LA at 110 °C. All the complexes showed considerable catalytic activity in mass/bulk and solvent polymerization as summarized in Table 3 and the kinetic plots are presented in Fig. 3. The activity of the complexes was compared within and across each triad since they differ basically in the electronic property of the ligand and co-ligand. The outcome of the experiment revealed that the polymerization rates relied on the inductive nature of the substituents on the benzoates within the triads while the induction time experienced by the complexes varied with the Schiff base ligand in the complex. For instance, complexes **7**, **8** and **9** containing an electron withdrawing substituent in the Schiff base ligand had an induction period of 30 min while complexes **1**, **4** and **6**, as well as **2**, **3** and **5** which possess electron donating groups on the ligand had an induction period of 4–6 h and about 18 h, respectively.

The complexes with unsubstituted benzoate co-ligands were the most active in their triad; with complex **4** having the maximum $k_{app}$ of 0.3450 h$^{-1}$ (Table 3, entry 5). A plausible reason for this observation can be traced to the lability of the Zn–O bond. Complexes containing the electron withdrawing fluoro group on the carboxylate ligand (Table 3, entries 4, 9 and 12) were more active than those with electron donating methyl group (Table 3, entries 3, 8 and 11) because they reduce the nucleophilicity at the metal center [56]. Complex **1** having two different zinc centers forming a rigid eight membered ring had a lower rate compared to the paddled-wheel conformation observed with complex **4**.

Complexes **4** and **7**, which are the most active for ε-CL polymerization were selected for polymerization of $_L$-LA and *rac*-LA in toluene under same conditions. The polymerization data and kinetic plots are provided in Table 3 and Fig. 4, respectively. The catalytic activity obtained with complex **7** was higher than that of complex **4** in the polymerization of *rac*-LA and $_L$-LA and the order was reversed for ε-CL. Both complexes afforded PLA of higher molecular weight with *rac*-LA (Table 3, entries 16 and 18) over $_L$-LA (Table 3, entries 15 and 17) whereas the $k_{app}$ for $_L$-LA is greater than for *rac*-LA. As observed in the polymerization of ε-CL, the induction time of complex **4** in the polymerization of *rac*-LA and $_L$-LA was again longer than that of complex **7** because of the bulky isopropyl substituent in complex **4** which is known to hinder monomer access and forthwith decreased the catalytic activity [22,57]. However, the molecular
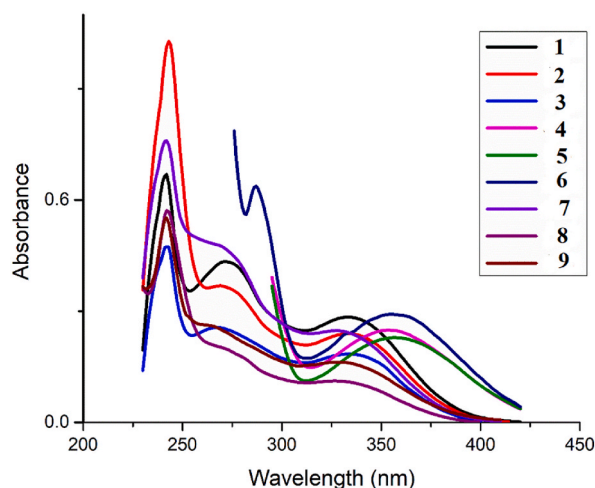


**Fig. 1.** UV–Vis spectra of complexes **1**–**9** in ~10⁻⁵ M DCM solutions.
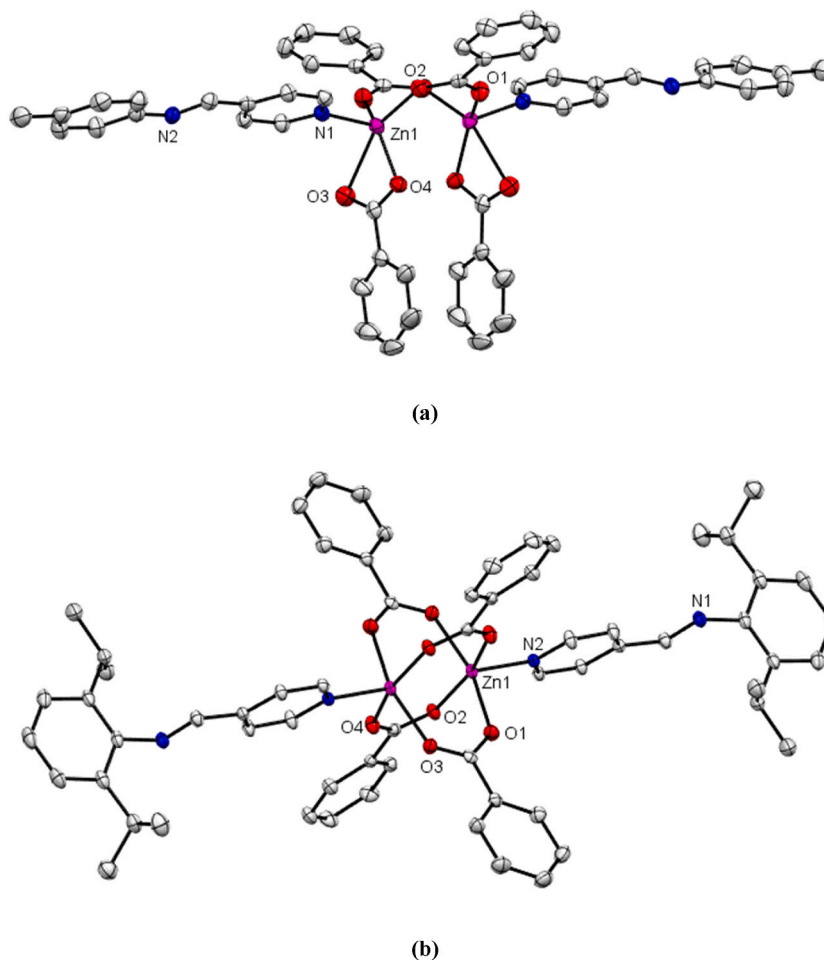
**(a)**



**(b)**

**Fig. 2.** ORTEP drawing of (a) complex **1** and (b) complex **4** with thermal ellipsoids drawn at 50% probability level. Hydrogen atoms are omitted for clarity.

**Table 2**
Selected bond lengths (Å) and bond angles (°) for complexes **1** and **4**.

| Complex | 1 | | 4 | |
|---|---|---|---|---|
| **Zn–O** | 1.9413 (11) | 1.9899 (12) | 2.0813 (12) | 2.0808 (12) |
| | 1.9547 (12) | 2.5542 (13) | 2.0624 (12) | 2.0792 (12) |
| **Zn—N$_{py}$** | 2.0375 (14) | | 2.0565 (13) | |
| **O–Zn–O** | 87.12 (5) | | 88.36 (5) | |
| | 132.06 (5) | | 89.05 (5) | |
| **O–Zn—N$_{py}$** | 93.26 (5) | | 96.99 (5) | |
| | 99.33 (5) | | | |
| | 109.78 (5) | | 102.66 (5) | |

Symmetry operators: i = 1 − x, +y, 3/2 −s z for **1**.

weights of polymers attained with complex **4** are greater than those furnished by complex **7** (Table 3).

## 6. Effect of solvent and alcohol initiators

The influence of external co-initiator (BnOH) was examined with complexes **1**, **4** and **7** using a [M]$_0$: [I]$_0$: [BnOH]$_0$ ratio of 200:1:1 at 110 °C (Fig. 5). The activities obtained after adding BnOH (Table 3, entries 2, 6 and 12) were higher than those obtained in its absence (Table 3, entries 1, 5 and 11). Similarly, the addition of ethanol as co-initiator to complex **4** increased catalytic activity (Table 3, entry 7). The remarkable increase in the catalytic activity with the addition of alcohol co-initiators is as a result of the production of alkoxides species which are known to increase the active sites [58]. However, the solution polymerization using complex

**Table 3**
Summary of polymerization data of $\varepsilon$-CL catalyzed by complexes **1–9**[a].

| Entry | Complex | t (h | [b]Conv (%) | [c]$M_{n(calcd)}$ (g mol$^{-1}$) | [b]$M_{n(NMR)}$ (g mol$^{-1}$) | [d]$M_{n(GPC)}$ (g mol$^{-1}$) | [d]Đ | $k_{app}$ (h$^{-1}$) |
|---|---|---|---|---|---|---|---|---|
| 1 | **1** | 29 | 98 | 22 371 | 3278 | 2950 | 1.95 | 0.1442 |
| 2 | [e]**1** | 10 | 98 | 22 371 | 2267 | – | – | 0.4144 |
| 3 | **2** | 49 | 98 | 22 371 | 3222 | 3848 | 1.86 | 0.1156 |
| 4 | **3** | 49 | 98 | 22 371 | 3162 | 3429 | 2.06 | 0.1173 |
| 5 | **4** | 15 | 99 | 22 599 | 2856 | 3160 | 1.95 | 0.3450 |
| 6 | [e]**4** | 6 | 99 | 22 599 | 1947 | – | – | 0.7626 |
| 7 | [f]**4** | 19 | 99 | 22 599 | 3137 | – | – | 0.1706 |
| 8 | [g]**4** | 5 | 98 | 22 371 | 1078 | – | – | 0.7806 |
| 9 | **5** | 48 | 98 | 22 371 | 3925 | 3811 | 2.19 | 0.1215 |
| 10 | **6** | 31 | 99 | 22 599 | 4144 | 4262 | 2.26 | 0.1782 |
| 11 | **7** | 15 | 97 | 22 143 | 3137 | – | – | 0.2369 |
| 12 | [e]**7** | 5 | 98 | 22 371 | 1076 | – | – | 0.7743 |
| 13 | **8** | 40 | 99 | 22 599 | 3586 | – | – | 0.1019 |
| 14 | **9** | 21 | 99 | 22 599 | 4175 | – | – | 0.2288 |
| 15 | [h]**4** | 40 | 99 | 22 599 | 3713 | 1285 | 1.72 | 0.1227 |
| 16 | [i]**4** | 40 | 99 | 22 599 | 5451 | 2760 | 2.05 | 0.1048 |
| 17 | [h]**7** | 40 | 99 | 22 599 | 2620 | – | – | 0.1389 |
| 18 | [i]**7** | 40 | 99 | 22 599 | 4109 | – | – | 0.115 |

[a] Polymerization conditions: [M]: [I] = 200:1, 110 °C, Bulk.
[b] Determined from NMR.
[c] $M_n$ calculated from the $M_{wt}$ of monomer x [M]$_0$: [I]$_0$ × Conv.,
[d] Obtained from GPC analysis and calibrated by polystyrene standard considering Mark-Houwink's corrections of 0.56 for PCL and 0.58 for PLAs.
[e] Benzyl alcohol.
[f] Toluene and.
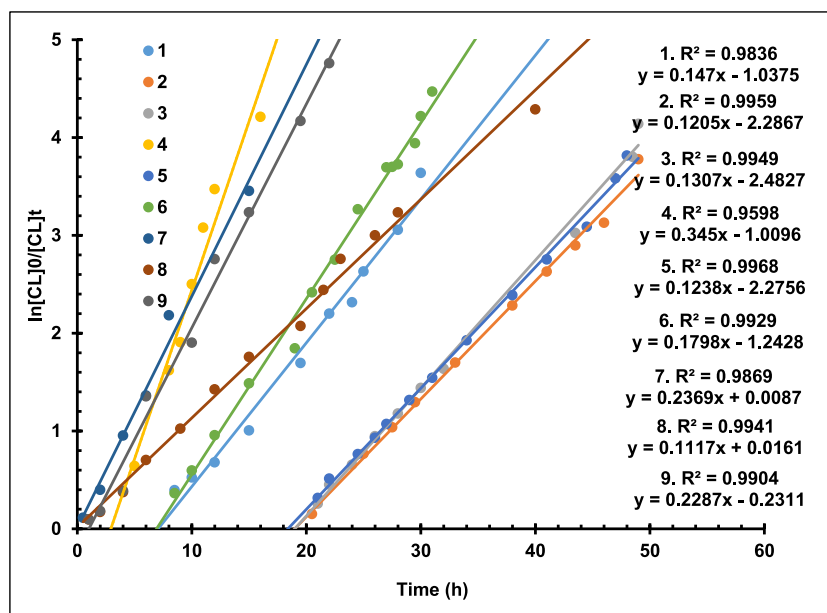[g] Ethanol.
[h] L-LA.
[i] rac-LA.



**Fig. 3.** Kinetic plots of ln [CL]$_0$/[CL]$_t$ *vs.* t for $\varepsilon$-CL polymerization in bulk using complexes **1–9** at 110 °C, [CL]$_0$: [I]$_0$ = 200.

**4** in toluene (Table 3, entry 8) resulted in a reduction of the catalytic rates compared to that obtained in bulk (Table 3, entry 5) because the concentration of reactive species involved in the polymerization reduced greatly, a phenomenon that has been reported in literature [25]. The $^1$H NMR spectrum of PCL and PLA obtained with complex **4**/alcohol systems shown in Fig. S34 and S35 confirmed a co-initiator-initiated ROP.
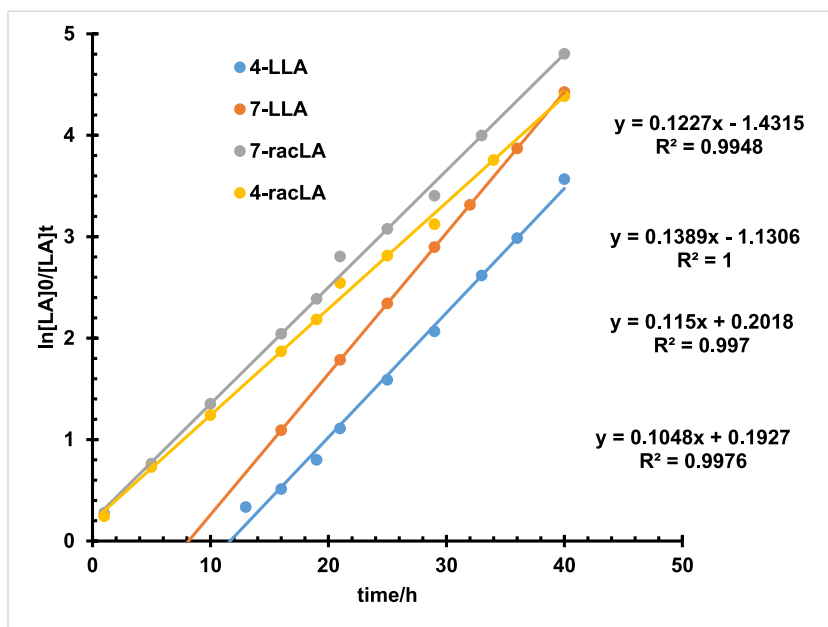
**Fig. 4.** Kinetic plots of ln $[LA]_0/[LA]_t$ *vs.* t for LA polymerization in bulk using complexes **4** and **7** at 110 °C, $[LA]_0 : [I]_0 = 200:1$.
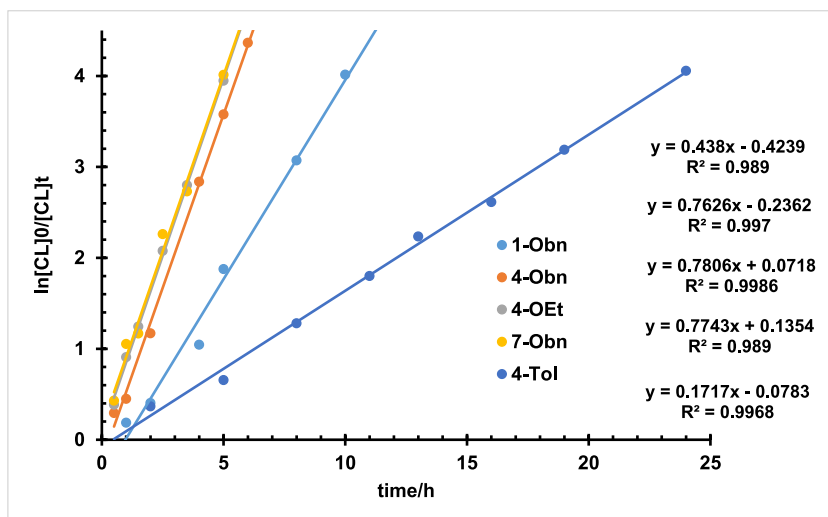


**Fig. 5.** Kinetic plots of ln $[CL]_0/[CL]_t$ *vs.* t for ε-CL polymerization in the presence of benzyl alcohol as initiator and toluene as solvent at 110 °C, $[CL]_0/[I]_0 = 200$.

## 7. Reaction order

The reaction order of complex **4** was examined by changing the catalyst concentration at a constant ε-CL concentration at 110 °C (Table 4)). From the semi-log kinetic plot (Fig. 6) for the metal complex studied, a linear relationship was observed, which corresponds

**Table 4**
Summary of polymerization data of ε-CL by complex **4** at different catalyst concentrations.

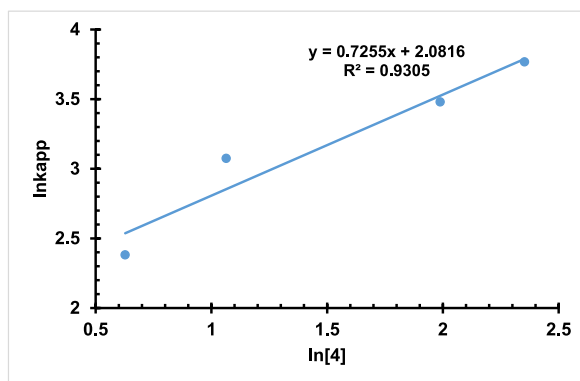| Entry | Complex | [M:I] | t(h) | [b]Conv (%) | [d]$M_{n(NMR)}$ | $k_{app}$ (h$^{-1}$) |
|---|---|---|---|---|---|---|
| 1 | 4 | 100 | 9 | 99 | 2689 | 0.5338 |
| 2 | 4 | 200 | 14 | 99 | 2856 | 0.3450 |
| 3 | 4 | 300 | 40 | 99 | 2903 | 0.1341 |
| 4 | 4 | 400 | 60 | 99 | 3131 | 0.0951 |

**Fig. 6.** Plot of ln$k_{app}$ against ln [**4**] for the determination of reaction order.

to *pseudo*-first order reaction kinetics. The polymerization rate is represented with equation (3) below;

$$\frac{d[\text{M}]}{dt} = k[\text{M}] \tag{3}$$

where $k = k_r\,[\text{C}]^y$, $k_r$ is the chain propagation rate, [C] is the initiator concentration and y, the reaction order.

An increase in $k_{app}$ as the catalyst concentration increased was observed, alluding to first order kinetics with respect to complex **4**. A linear plot of ln$k_{app}$ *vs.* ln [**4**] was obtained and the gradient of the line of best fit corresponds to the order of reaction (Fig. 6). The order with respect to complex **4** was found to be 0.7255 ≈ 0.7 and the rate law is represented by equation (4). The fractional order obtained with catalyst/initiator in melt polymerization is in tandem with literature reports which suggests an accumulation and dissociation of the active groups in the ROP reaction [32,59–61]. The $^1$H NMR analysis of the polymer revealed a rise in polymer molecular weight from 2689 g mol$^{-1}$ to 3131 g mol$^{-1}$ as the monomer to catalyst ratio was changed from 100:1 to 400:1.

$$\frac{d[\text{CL}]}{dt} = k[\text{CL}][\textbf{4}]^{0.7} \tag{4}$$

### 7.1. Effect of temperature on ε-CL polymerization

The mass polymerization of ε-CL was further investigated by complex **4** between 80 °C and 110 °C to obtain the activation parameters. The results presented in Table 5 showed that the temperature significantly influenced the catalytic rate obtained. At low temperature a semi-log plot of ln [CL]$_0$/[CL]$_t$ *vs.* time exhibit an extended induction period before a gradual linear increase in rate, and there is a ten-fold decrease in $k_{app}$ from 0.345 h$^{-1}$ to 0.0355 as the temperature is changed from 110 °C to 80 °C.

The conversion and molecular weight of PCL obtained at lower temperature were comparably lower than those obtained at elevated temperature. The curves in the chromatogram of PCL obtained from SEC analysis revealed a mono-modal pattern displayed at all the temperatures examined suggest that the polymerization was initiated by similar active sites [62,63]. Although the catalytic activity and obtained molecular weights of PCL increased at higher temperatures, the broadness of their curves is an indication of intra- and inter-molecular transesterification reactions which results in broad polymer dispersity (Fig. 7).

The energy barrier ($E_a$) of 86.89 kJ mol$^{-1}$ was deduced from Arrhenius equation (5) from the gradient of the fitted line of the relationship between ln$k$ and the inverse of the polymerization temperature (1/T) (Fig. 8). From the Eyring equation (6) the computed thermodynamic parameters are enthalpy ($\Delta H^\#$) 83.84 kJ mol$^{-1}$ and entropy ($\Delta S^\#$) 105.49 J K$^{-1}$ mol$^{-1}$ (Fig. 8). These activation parameters obtained conforms to an organized transition state corresponding to a coordination-insertion mechanism.

$$\ln k = \ln A + \frac{-E_a}{RT} \tag{5}$$

$$\ln\left(\frac{K_{app}}{T}\right) = \frac{-\Delta H^\#}{R}\frac{1}{T} + \ln\frac{K_b}{h} + \frac{\Delta S^\#}{R} \tag{6}$$

#### 7.1.1. GPC molecular weight and molecular weight distribution of polymers

Corrected GPC molecular weights ($M_n$) and poly dispersity index (Đ) of chosen catalysts are comparable to those obtained from $^1$H NMR (Table 3) with only a few variations. Low molecular weight polymers of 2950–4262 g mol$^{-1}$ and 1285–2760 g mol$^{-1}$ were obtained from GPC analysis for PCL and PLAs, respectively. Dispersity between 1.80 – 2.26 and 1.72–2.05 recorded for PCL and PLAs, respectively, presupposes the presence of intra- and inter-molecular *trans*-esterification reactions. The steric and electronic properties of the Schiff base and carboxylate ligands in the complexes influenced the $M_n$ obtained from GPC analysis. For instance, complexes **4–6** with *ortho* bulky isopropyl substituent gave $M_n$ of 3160 g mol$^{-1}$ (**4**, unsubstituted) < 3811 g mol$^{-1}$ (**5**, electron donating) < 4262 g mol$^{-1}$ (**6**, electron withdrawing). A slight deviation in the above trend was recorded for complexes **1–3** containing a less bulky

**Table 5**
Data for ε-CL polymerization at different temperatures catalyzed by complex **4**[a].

| Entry | Complex | [M:I] | t(h) | [b]Conv (%) | [b]$M_{n(NMR)}$ | [c]$M_{n(GPC)}$ | [c]Đ | $k_{app}$ (h$^{-1}$) |
|-------|---------|-------|------|-------------|------------------|------------------|------|----------------------|
| 1 | [d]**4** | 200 | 90 | 95 | 2000 | – | – | 0.0335 |
| 2 | [e]**4** | 200 | 62 | 99 | 2284 | 2152 | 1.58 | 0.0700 |
| 3 | [f]**4** | 200 | 33 | 99 | 2514 | 2304 | 1.80 | 0.1473 |
| 4 | [g]**4** | 200 | 15 | 99 | 2856 | 3160 | 1.95 | 0.3450 |

[a] Polymerization conditions: 110 °C, Bulk.
[b] Determined from NMR.
[c] Obtained from GPC analysis and calibrated by polystyrene standard considering Mark-Houwink's corrections of 0.56 for PCL.
[d] 80 °C.
[e] 90 °C.
[f] 100 °C.
[g] 110 °C.
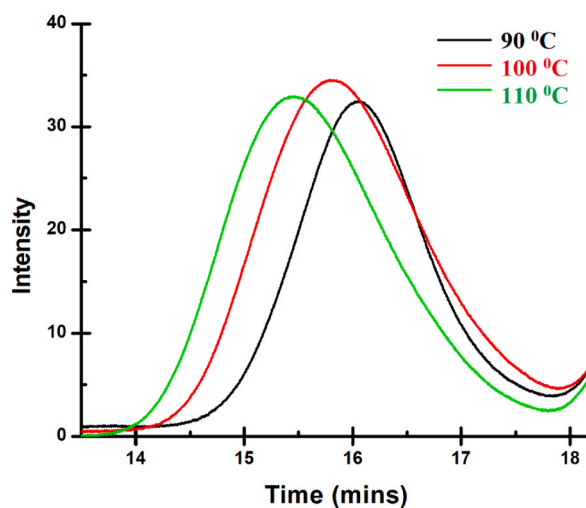


**Fig. 7.** An overlay of the GPC chromatogram of PCL obtained by **4** at different temperatures.
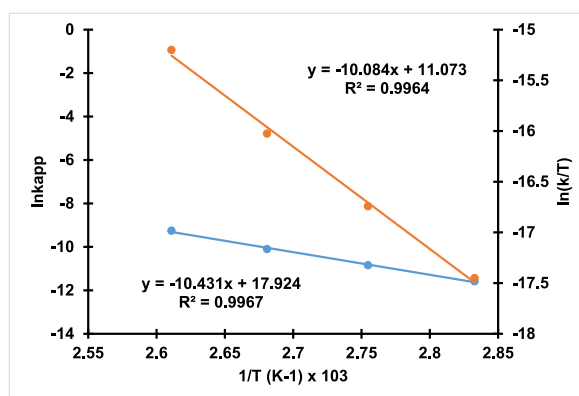


**Fig. 8.** Arrhenius and Eyring plot for the bulk polymerization of ε-CL initiated by **4**.

substituent; where complex **2** (electron donating) had a slightly higher $M_n$ of 3848 g mol$^{-1}$ than $M_n$ of 3429 g mol$^{-1}$ obtained for **3** (electron withdrawing) while **1** (unsubstituted) remained the least in the triad with $M_n$ of 2950 g mol$^{-1}$ which is traceable to the distorted tetrahedral geometry.

## 7.2. End group analysis and reaction mechanism

End groups of polymers obtained with complexes **4** and **7** at 110 °C using a $[M]_0$: $[I]_0$ ratio of 200:1 were analyzed with $^1$H NMR (Fig. S34 and S35) and ESI-MS (Fig. S36). The results support a coordination insertion mechanism as proposed in Fig. 9. The process of monomer enchainment begins by monomer activation at the metal active site. This is preceded by scission of the monomer acyl-oxygen linkage *via* insertion in the M—O bond. The ancillary organic ligand stay connected to the catalytic center controlling the activity, polymer molecular weights and molecular weights distributions, monomer addition and stereochemistry. Finally, the propagation is terminated by hydrolysis, where the metal is dislodged from the growing chain giving hydroxyl end capped polymers [22,34]. When benzyl alcohol was included as a co-initiator, the $^1$H NMR spectrum of PCL (Fig. S34) revealed additional methylene proton (g, 5.12 ppm) and aromatic proton (h, 7.37 ppm) peaks signifying generation of alkoxide initiating species (BnO⁻) responsible initiating of the polymerization reaction *via* a coordination insertion pathway.

## 8. Stereochemistry of poly-lactides

The thermal and mechanical behavior of synthesized PLA is informed by their microstructure, which is determined by the positioning of methyl groups on the lactides (L-LA, D-LA, *rac*-LA and *meso*-LA), and the chirality of the catalyst employed. Homo-nuclear decoupled $^1$H and $^{13}$C NMR was employed for the microstructural analysis of the synthesized PLA and the tetrad sequence were assigned according to established reports for PLA in literature [64,65]. The homo-nuclear decoupled $^1$H NMR spectra of poly (L-LA) revealed an essentially isotactic PLA whereas the poly (*rac*-LA) points to an isotactic stereo-*block* microstructural conformation (Fig. S37, S38, S39 and S40). The singular methine and carbonyl carbon $^{13}$C NMR peaks of poly (L-LA) obtained by **4** at 69.03 and 169.61 ppm, respectively, confirms the isotactic nature of the PLA (Fig. S41a and S42bESI).

However, two methine carbon peaks were observed at 69.19 ppm and 69.02 ppm for poly (*rac*-LA) were assigned to *mrm* and (*mmm, mmr, mrr, rmr*) sequences (Fig. S41bESI). More so, carbonyl carbon peaks at 169.61 ppm, 169.33–169.42 ppm and 169.16 ppm are assigned to *rr*, (*rm, mr*) and *mm* configurations (Fig. S42bESI) [34,65,66]. The physicochemical properties of the synthesized PLA examined by thermal analysis using DSC-TGA is summarized in Table 6. The thermogram had melting temperatures ($T_m$) between 116.58 and 188.03 °C (Fig. S43) [67]. The detected decomposition temperatures between 278.78 °C and 331.32 °C is suggestive of an isotactic PLA with a metal capped end, which began to decompose at 214.74 °C till the maximum decomposition temperature ($T_{max}$) at 436.01 °C resulting in a $T_{decomp}$ of 221.27 °C (Fig. S43).

## 9. Conclusion

Nine Zn(II) carboxylate complexes of 4-pyridinyl Schiff base ligands were obtained from a room temperature reaction of Zn(II) acetate with the Schiff base and carboxylate ligands. Their geometry and coordination were established by spectroscopic studies (FTIR, NMR and mass spectroscopy) and elemental analysis. The crystal structures of complexes **1** and **4** were ascertained by single crystal X-ray diffraction studies to be dinuclear with the Schiff base ligands coordinating in an unidentate manner. On the one hand, the carboxylate co-ligands in complex **1** coordinated in monodentate and bridging modes resulting in a distorted tetrahedral geometry around each Zn(II) centers while all the carboxylate co-ligands in complex **4** coordinated in a bridging mode occasioning a paddle wheel arrangement on the Zn(II) atoms. The Zn(II) complexes were catalytic active towards the polymerization of ε-CL, L-LA and *rac*-LA affording low molecular weight polymers with or without alcohol initiators. Ligand and co-ligand electronic and steric effects significantly influenced the catalytic activity of the complexes. Homo-nuclear decoupled $^1$H NMR and DSC-TGA analysis of the
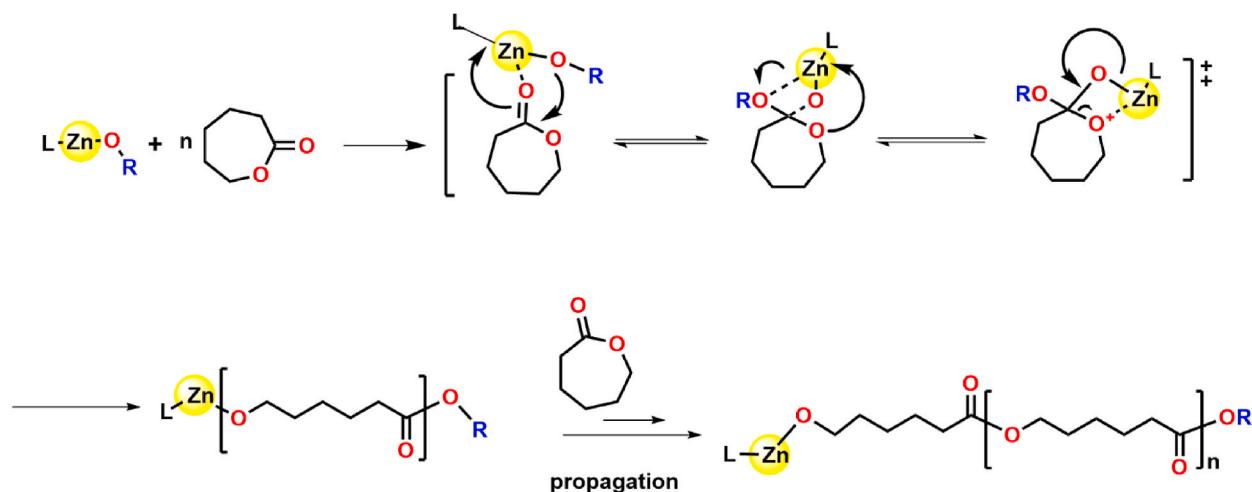


**Fig. 9.** Proposed mechanism for the ROP of ε-CL.

**Table 6**

TGA data for poly (L-LA) and poly (*rac*-LA) synthesized by complexes **4** and **7**[a].

| Entry | Onset (°C) | 50% (°C) | $T_{max}$ (°C) | $\Delta T_{decomp}$ (°C) | $T_m$ (°C) |
|---|---|---|---|---|---|
| [b]L-LA | 201.6 | 304.3 | 410.5 | 208.9 | 142.96 |
| [b]*rac*-LA | 214.7 | 326.4 | 436.1 | 221.4 | 188.03 |
| [c]L-LA | 179.7 | 268.2 | 402.5 | 222.8 | 116.58 |
| [c]*rac*-LA | 181.9 | 282.7 | 398.2 | 216.3 | 144.41 |

[a] Heating rate of 10 °C/min.
[b] Complex **4** and.
[c] Complex **7**.

synthesized PLA revealed an isotactically enriched PLA.

## Declaration

*Author contribution statement*

Damilola C. Akintayo: Conceived and designed the experiments; Performed the experiments; Analyzed and interpreted the data; Wrote the paper. Wisdom A. Munzeiwa: Conceived and designed the experiments; Analyzed and interpreted the data. Sreekantha B. Jonnalagadda, Bernard Omondi: Conceived and designed the experiments; Analyzed and interpreted the data; Contributed reagents, materials, analysis tools or data.

*Data availability statement*

The data that support the findings of this study are openly available in Cambridge Crystallographic Data Centre at http://www.ccdc.cam.ac.uk/conts/retrieving.html, or *via* e-mail: deposit@ccdc.cam.ac.uk, reference number (CCDC 2191381–2191382).

*Declaration of interest's statement*

The authors declare no competing interests.

## Appendix A. Supplementary data

Supplementary data related to this article can be found at https://doi.org/10.1016/j.heliyon.2023.e13514.
This is a provisional file, not the final typeset article.

## References

[1] M. Kashif, B.-M. Yun, K.-S. Lee, Y.-W. Chang, Biodegradable shape-memory poly(ε-caprolactone)/polyhedral oligomeric silsequioxane nanocomposites: sustained drug release and hydrolytic degradation, Mater. Lett. 166 (2016) 125–128.

[2] L. Lin, Y. Xu, S. Wang, M. Xiao, Y. Meng, Ring-opening polymerization of l-lactide and ε-caprolactone catalyzed by versatile tri-zinc complex: synthesis of biodegradable polyester with gradient sequence structure, Eur. Polym. J. 74 (2016) 109–119.

[3] L. Lamch, J. Kulbacka, J. Pietkiewicz, J. Rossowska, M. Dubinska-Magiera, A. Choromanska, K.A. Wilk, Preparation and characterization of new zinc(II) phthalocyanine — containing poly(l-lactide)-b-poly(ethylene glycol) copolymer micelles for photodynamic therapy, J. Photochem. Photobiol. B Biol. 160 (2016) 185–197.

[4] N. Jurgensen, J. Zimmermann, A.J. Morfa, G. Hernandez-Sosa, Biodegradable polycaprolactone as ion solvating polymer for solution-processed light-emitting electrochemical cells, Sci. Rep. 6 (2016) 36643–36648.

[5] C. Zhang, Biodegradable Polyesters: Synthesis, Properties, Applications, Biodegradable Polyesters, Wiley-VCH, Weinheim, 2015.

[6] R.T. Mathers, M.A.R. Meier, Green Polymerization Methods: Renewable Starting Materials, Catalysis and Waste Reduction, Wiley-VCH Verlag, Weinheim, Germany, 2011.

[7] S. Inkinen, M. Hakkarainen, A.-C. Albertsson, A. Sodergard, From lactic acid to poly(lactic acid) (PLA): characterization and analysis of PLA and its precursors, Biomacromolecules 12 (2011) 523–532.

[8] T.J.J. Whitehorne, F. Schaper, Square-planar Cu(II) diketiminate complexes in lactide polymerization, Inorg. Chem. 52 (2013) 13612–13622.

[9] A.C. Albertsson, I.K. Varma, Recent developments in ring opening polymerization of lactones for biomedical applications, Biomacromolecules 4 (2003) 1466–1486.

[10] R. Auras, B. Harte, S. Selke, An overview of polylactides as packaging materials, Macromol. Biosci. 4 (2004) 835–864.

[11] Z. Zhong, P.J. Dijkstra, C. Birg, M. Westerhausen, J. Feijen, A novel and versatile calcium-based initiator system for the ring-opening polymerization of cyclic esters, Macromolecules 34 (2001) 3863–3868.

[12] L.-C. Liang, S.-T. Lin, C.-C. Chien, Lithium complexes of tridentate amine biphenolate ligands containing distinct N-alkyl substituents, Polyhedron 52 (2013) 1090–1095.

[13] M.H. Chisholm, K. Choojun, J.C. Gallucci, P.M. Wambua, Chemistry of magnesium alkyls supported by 1,5,9-trimesityldipyrromethene and 2-[(2,6-diisopropylphenyl)amino]-4-[(2,6-diisopropylphenyl)imino]pent-2-ene. A comparative study, Chem. Sci. 3 (2012) 3445–3457.

[14] A. Balaji, M.V. Vellayappan, A.A. John, A.P. Subramanian, S.K. Jaganathan, M. Selva Kumar, A.A.b. Mohd Faudzi, E. Supriyanto, M. Yusof, Biomaterials based nano-applications of Aloe vera and its perspective: a review, RSC Adv. 5 (2015) 86199–86213.

[15] A. Kowalski, A. Duda, S. Penczek, Mechanism of cyclic ester polymerization initiated with Tin(II) octoate. 2. Macromolecules fitted with Tin(II) alkoxide species observed directly in MALDI−TOF spectra, Macromolecules 33 (2000) 689–695.

[16] C. Fliedel, V. Rosa, F.M. Alves, A.M. Martins, T. Aviles, S. Dagorne, P. O-Phosphinophenolate, zinc(II) species: synthesis, structure and use in the ring-opening polymerization (ROP) of lactide, ε-caprolactone and trimethylene carbonate, Dalton Trans. 44 (2015) 12376–12387.

[17] E. Faggi, R. Gavara, M. Bolte, L. Fajari, L. Julia, L. Rodriguez, I. Alfonso, Copper(II) complexes of macrocyclic and open-chain pseudopeptidic ligands: synthesis, characterization and interaction with dicarboxylates, Dalton Trans. 44 (2015) 12700–12710.

[18] M.J.L. Tschan, J. Guo, S.K. Raman, E. Brule, T. Roisnel, M.-N. Rager, R. Legay, G. Durieux, B. Rigaud, C.M. Thomas, Zinc and cobalt complexes based on tripodal ligands: synthesis, structure and reactivity toward lactide, Dalton Trans. 43 (2014) 4550–4564.

[19] X. Hu, C. Lu, B. Wu, H. Ding, B. Zhao, Y. Yao, Q. Shen, Synthesis and structural diversity of lanthanide amidate complexes and their catalytic activities for the ring-opening polymerization of *rac*-lactide, J. Organomet. Chem. 732 (2013) 92–101.

[20] A. Bhaw-Luximon, D. Jhurry, S. Motala-Timol, Y. Lochee, Polymerization of ε-caprolactone and its copolymerization with γ-butyrolactone using metal complexes, Macromolecules 231 (2006) 60–68.

[21] J. Ling, J. Shen, T.E. Hogen-Esch, A density functional theory study of the mechanisms of scandium-alkoxide initiated coordination–insertion ring-opening polymerization of cyclic esters, Polymer 50 (2009) 3575–3581.

[22] B.J. O'Keefe, L.E. Breyfogle, M.A. Hillmyer, W.B. Tolman, Mechanistic comparison of cyclic ester polymerizations by novel iron (III)− alkoxide complexes: single vs multiple site catalysis, J. Am. Chem. Soc. 124 (2002) 4384–4393.

[23] N. Buis, S.A. French, G.D. Ruggiero, B. Stengel, A.A.D. Tulloch, I.H. Williams, Computational investigation of mechanisms for ring-opening polymerization of ε-caprolactone: evidence for bifunctional catalysis by alcohols, J. Chem. Theor. Comput. 3 (2007) 146–155.

[24] S.O. Ojwach, T.T. Okemwa, N.W. Attandoh, B. Omondi, Structural and kinetic studies of the polymerization reactions of ?-caprolactone catalyzed by (pyrazol-1-ylmethyl)pyridine Cu(ii) and Zn(ii) complexes, Dalton Trans. 42 (2013) 10735–10745.

[25] S.O. Ojwach, T.T. Okemwa, N.W. Attandoh, B. Omondi, Structural and kinetic studies of the polymerization reactions of ε-caprolactone catalyzed by (pyrazol-1-ylmethyl)pyridine Cu(II) and Zn(II) complexes, Dalton Trans. 42 (2013) 10735–10745.

[26] S.O. Ojwach, T.P. Zaca, Ring-opening polymerization of lactides by (Pyrazol-1-ylmethyl)pyridine Zn(II) and Cu(II) complexes: kinetics, mechanism and tacticity studies, S. Afr. J. Chem. 68 (2015) 7–U21.

[27] M. Zikode, S.O. Ojwach, M.P. Akerman, Structurally rigid bis(pyrazolyl)pyridine Zn(II) and Cu(II) complexes: structures and kinetic studies in ring-opening polymerization of ε-caprolactone, Appl. Organomet. Chem. 31 (2016), e3556.

[28] M. Zikode, S.O. Ojwach, M.P. Akerman, Bis(pyrazolylmethyl)pyridine Zn(II) and Cu(II) complexes: molecular structures and kinetic studies of ring-opening polymerization of ε-caprolactone, J. Mol. Catal. Chem. 413 (2016) 24–31.

[29] D. Appavoo, B. Omondi, I.A. Guzei, J.L. van Wyk, O. Zinyemba, J. Darkwa, Bis(3,5-dimethylpyrazole) copper(II) and zinc(II) complexes as efficient initiators for the ring opening polymerization of ε-caprolactone and D,L-lactide, Polyhedron 69 (2014) 55–60.

[30] N.W. Attandoh, S.O. Ojwach, O.Q. Munro, (Benzimidazolylmethyl)amine Zn(II) and Cu(II) arboxylate complexes: structural, mechanistic and kinetic studies of polymerisation reactions of ε-caprolactone, Eur. J. Inorg. Chem. 2014 (2014) 3053–3064.

[31] E.D. Akpan, S.O. Ojwach, B. Omondi, V.O. Nyamori, Zn(II) and Cu(II) formamidine complexes: structural, kinetics and polymer tacticity studies in the ring-opening polymerization of ε-caprolactone and lactides, New J. Chem. 40 (2016) 3499–3510.

[32] E.D. Akpan, S.O. Ojwach, B. Omondi, V.O. Nyamori, Structural and kinetic studies of the ring-opening polymerization of cyclic esters using N,N′ diarylformamidines Zn(II) complexes, Polyhedron 110 (2016) 63–72.

[33] W.A. Munzeiwa, B. Omondi, V.O. Nyamori, Synthesis and polymerization kinetics of ε-caprolactone and L-lactide to low molecular weight polyesters catalyzed by Zn(II) and Cu(II) N-hydroxy-N,N′-diarylformamidine complexes, Polyhedron 138 (2017) 295–305.

[34] W.A. Munzeiwa, V.O. Nyamori, B. Omondi, Zn(II) and Cu(II) unsymmetrical formamidine complexes as effective initiators for ring-opening polymerization of cyclic esters, Appl. Organomet. Chem. 32 (2018).

[35] F. Naz, F. Mumtaz, S. Chaemchuen, F. Verpoort, Bulk ring-opening polymerization of ε-caprolactone by zeolitic imidazolate framework, Catal. Lett. 149 (2019) 2132–2141.

[36] N.R. Rightmire, T.P. Hanusa, Advances in organometallic synthesis with mechanochemical methods, Dalton Trans. 45 (2016) 2352–2362.

[37] T. Abe, A. Miyazawa, Y. Kawanishi, H. Konno, Microwave-assisted synthesis of metal complexes, Mini-Reviews Org. Chem. 8 (2011) 315–333.

[38] A. Beillard, X. Bantreil, T.-X. Metro, J. Martinez, F. Lamaty, Alternative technologies that facilitate access to discrete metal complexes, Chem. Rev. 119 (2019) 7529–7609.

[39] D.C. Akintayo, W.A. Munzeiwa, S.B. Jonnalagadda, B. Omondi, Ring-opening polymerization of cyclic esters by 3-and 4-pyridinyl Schiff base Zn (II) and Cu (II) paddlewheel complexes: kinetic, mechanistic and tacticity studies, Arab. J. Chem. 14 (2021) 103313.

[40] R. Sarma, D. Kalita, J.B. Baruah, Solvent induced reactivity of 3,5-dimethylpyrazole towards zinc (II) carboxylates, Dalton Trans. (2009) 7428–7436.

[41] D.C. Akintayo, W.A. Munzeiwa, S.B. Jonnalagadda, B. Omondi, Influence of nuclearity and coordination geometry on the catalytic activity of Zn (II) carboxylate complexes in ring-opening polymerization of ε-caprolactone and lactides, Inorg. Chim. Acta. 532 (2022), 120715.

[42] D.C. Akintayo, W.A. Munzeiwa, S.B. Jonnalagadda, B. Omondi, N3/4-pyridinyl Schiff base copper (II) benzoate complexes: synthesis, crystal structures and ring-opening polymerization studies, Transit. Met. Chem. 47 (2022) 113–126.

[43] Bruker, SAINT, SAINT Bruker AXS Inc, Madison, Wisconsin, USA, 2009.

[44] Bruker, SADABS, Bruker SADABS Bruker AXS Inc, Madison,Wisconsin, USA, 2009.

[45] O.V. Dolomanov, L.J. Bourhis, R.J. Gildea, J.A.K. Howard, H. Puschmann, OLEX2: a complete structure solution, refinement and analysis program, J. Appl. Crystallogr. 42 (2009) 339–341.

[46] G. Sheldrick, Shelx, Acta Crystallogr Sect. A: Found. Crystallogr. 64 (2008) 112–122.

[47] A.L. Garay, A. Pichon, S.L. James, Solvent-free synthesis of metal complexes, Chem. Soc. Rev. 36 (2007) 846–855.

[48] B.-H. Ye, X.-Y. Li, I.D. Williams, X.-M. Chen, Synthesis and structural characterization of di- and tetranuclear zinc complexes with phenolate and carboxylate bridges. Correlations between $^{13}$C NMR chemical shifts and carboxylate binding modes, Inorg. Chem. 41 (2002) 6426–6431.

[49] C. Obuah, Y. Lochee, J.H.L. Jordaan, D.P. Otto, T. Nyokong, J. Darkwa, (Ferrocenylpyrazolyl)zinc(II) benzoates as catalysts for the ring opening polymerization of ε-caprolactone, Polyhedron 90 (2015) 154–164.

[50] M. Premkumar, D. Kaleeswaran, G. Kaviyarasan, D.A. Prasanth, G. Venkatachalam, Mono and dinuclear Cu(II) carboxylate complexes with pyridine and 1-methylimidazole as Co–Ligands: synthesis, structure, antibacterial activity and catalytic nitroaldol reactions, ChemistrySelect 4 (2019) 7507–7511.

[51] A. Karmakar, I. Goldberg, Flexible porphyrin tetracarboxylic acids for crystal engineering, CrystEngComm 12 (2010) 4095–4100.

[52] N.W. Alcock, J. Culver, S.M. Roe, Secondary bonding. Part 15. Influence of lone pairs on co-ordination: comparison of diphenyl-tin(IV) and -tellurium(IV) carboxylates and dithiocarbamates, J. Chem. Soc., Dalton Trans. (1992) 1477–1484.

[53] P.D. Knight, A.J. White, C.K. Williams, Dinuclear zinc complexes using pentadentate phenolate ligands, Inorg. Chem. 47 (2008) 11711–11719.

[54] P. Maiti, A. Khan, T. Chattopadhyay, S. Das, K. Manna, D. Bose, S. Dey, E. Zangrando, D. Das, Dinuclear zinc (II) complexes with compartmental ligands: syntheses, structures, and bioactivities as artificial nuclease, J. Coord. Chem. 64 (2011) 3817–3831.

[55] G. Parkin, Synthetic analogues relevant to the structure and function of zinc enzymes, Chem. Rev. 104 (2004) 699–768.

[56] P. Hormnirun, E.L. Marshall, V.C. Gibson, R.I. Pugh, A.J.P. White, Study of ligand substituent effects on the rate and stereoselectivity of lactide polymerization using aluminum salen-type initiators, Proc. Natl. Acad. Sci. USA 103 (2006) 15343–15348.

[57] D.J. Hodgson, Structural characterization of the binuclear copper(II) complex {3,3′-dimethoxy-4,4′-bis(3-methyltriazene-3-oxide)biphenyl}di-copper(II), Inorg. Chim. Acta. 75 (1983) 225–228.

[58] N. Ikpo, C. Hoffmann, L.N. Dawe, F.M. Kerton, Ring-opening polymerization of epsilon-caprolactone by lithium piperazinyl-aminephenolate complexes: synthesis, characterization and kinetic studies, Dalton Trans. 41 (2012) 6651–6660.

[59] S. Schmidt, S. Schulz, D. Blaser, R. Boese, M. Bolte, Synthesis and structural characterization of new zinc amidinate complexes, Organometallics 29 (2010) 6097–6103.

[60] P. Dubois, C. Jacobs, R. Jerome, P. Teyssie, Macromolecular engineering of polylactones and polylactides. 4. Mechanism and kinetics of lactide homopolymerization by aluminum isopropoxide, Macromolecules 24 (1991) 2266–2270.

[61] Y. Huang, W. Wang, C.-C. Lin, M.P. Blake, L. Clark, A.D. Schwarz, P. Mountford, Potassium, Zinc, and Magnesium complexes of a bulky OOO-tridentate bis (phenolate) ligand: synthesis, structures, and studies of cyclic ester polymerisation, Dalton Trans. 42 (2013) 9313–9324.

[62] C.G. Pitt, T.A. Marks, A. Schindler, Biodegradable Drug Delivery Systems Based on Aliphatic Polyesters: Application to Contraceptives and Narcotic Antagonists, Academic Press, NY, USA, 1980.

[63] J.M. Contreras, D. Medina, F. Lopez-Carrasquero, R.R. Contreras, Ring-opening polymerization of ε-caprolactone initiated by samarium acetate, J. Polym. Res. 20 (2013) 244.

[64] K.A.M. Thakur, R.T. Kean, E.S. Hall, J.J. Kolstad, T.A. Lindgren, M.A. Doscotch, J.I. Siepmann, E.J. Munson, High-Resolution $^{13}$C and $^1$H solution NMR study of poly(lactide), Macromolecules 30 (1997) 2422–2428.

[65] M.H. Chisholm, S.S. Iyer, D.G. McCollum, M. Pagel, U. Werner-Zwanziger, Microstructure of poly(lactide). phase-sensitive HETCOR spectra of poly(*meso*-lactide), poly(*rac*-lactide), and atactic poly(lactide), Macromolecules 32 (1999) 963–973.

[66] F. Chabot, M. Vert, S. Chapelle, P. Granger, Configurational structures of lactic acid stereocopolymers as determined by $^{13}$C-($^1$H) NMR, Polymer 24 (1983) 53–59.

[67] R. Petrus, P. Sobota, Zinc complexes supported by methyl salicylato ligands: synthesis, structure, and application in ring-opening polymerization of ʟ-lactide, Dalton Trans. 42 (2013) 13838–13844.